A Compact Wideband Dielectric Resonator Antenna with a Meandered Slot Ring and Cavity Backing

Citation for published version:
Podilchak, S, Johnstone, JC, Caillet, M, Clénet, M & Antar, YMM 2016, 'A Compact Wideband Dielectric Resonator Antenna with a Meandered Slot Ring and Cavity Backing', *IEEE Antennas and Wireless Propagation Letters*, vol. 15, pp. 909-913. https://doi.org/10.1109/LAWP.2015.2480547

Digital Object Identifier (DOI):
10.1109/LAWP.2015.2480547

Published In:
IEEE Antennas and Wireless Propagation Letters

A Compact Wideband Dielectric Resonator Antenna with a Meandered Slot Ring and Cavity Backing

Symon K. Podilchak, *Member, IEEE,* Jonathan C. Johnstone, Mathieu Caillet, Michel Clénet, *Senior Member, IEEE,* and Yahia M. M. Antar, *Life Fellow, IEEE*

***Abstract*—We design a compact cavity-backed antenna structure where a dielectric resonator (DR) element is surrounded by a meandered circular slot ring to enhance radiation efficiency. The DR for the antenna is cylindrical in shape and four degenerate $HE_{11\delta}$ modes are excited and driven by four, quadrature fed aperture coupled slots. Such a compact implementation hybridizes operation of the DR with the minturized ring as well as the four aperture coupled slots for circular polarization. Measured realized gain values are greater than 5 dBic from 1.14 GHz to 1.55 GHz defining a bandwidth of more than 30%. In addition, the half-power and 3 dB axial ratio beamwidths were measured to be more than 100° and 200°, respectively. The proposed design technique to employ such a secondary meandered slot ring may also be useful to improve antenna gain, bandwidth, and efficiency for other antenna and array structures.**

***Index Terms*—Broadband antennas, compact antennas, circular polarization (CP), dielectric resonator (DR), slot antenna.**

I. INTRODUCTION

MODERN radar systems and communication applications typically require compact antenna hardware that offers circularly polarized (CP) radiation such that, regardless of the orientation of the receive or transmit antennas, principal communication links can be maintained. Moreover, many conventional CP antenna structures and arrays offering broadband operation and high gain can have dimensions which are on the order of half a free-space wavelength or more, making them undesirable for compact implementations. Thus antenna miniaturization, while still maintaining reasonable bandwidth (BW) with minimal gain variation, is a challenging topic and of considerable interest within the electromagnetics community.

Dielectric resonator antennas (DRAs) are well adopted to overcome this miniaturization problem because their dielectric constant can be quite large which allows for physically smaller radiating elements when compared to conventional half-wavelength antennas operating in the same frequency band [1]-[3]. One technique to generate CP radiation over a broad BW using a multifeed system was proposed in [4] using a single dielectric resonator (DR) element having a dielectric constant of 9.5. In that work four vertical strip excitations were used for radiation and one power divider and two 90° hybrid couplers defined the feeding network. A 3 dB axial ratio BW of 25.9% was reported from 1.65 to 2.14 GHz. In [5] a more planar feed system with aperture coupled slots (ACSs) and a compact $0.75\lambda_0$ by $0.75\lambda_0$ ground plane was implemented for a CP BW of 36.2% with a centre frequency of about 1.4 GHz. Then in [6] a trapezoidally shaped DRA was investigated where a single inclined slot with microstrip feeding was employed to excite multiple resonant modes with close resonance frequencies across the passband (3.11 to 3.86 GHz) for a CP BW of 21.5%. A more simple square DRA was also studied in [7] that offered a 14% CP BW (centered at 3.5 GHz) using a vertical feed and parasitic copper strip open half-loops. Then in [8] a 50% CP BW was observed using a rectangular DR ring within a host dielectric substrate. To achieve CP radiation in that work, a metalic strip loop element, connected to the ground plane, was wrapped around the DR as an open conducting ring. A gain variation from 3.6 to 6.6 dBic was observed from about 3.5 to 5.7 GHz defining a bandwidth of 47.8%. The antenna size compared to the wavelength at 5.7 GHz was $0.53\lambda_0$ by $0.65\lambda_0$ by $0.10\lambda_0$.

In this letter we propose a new antenna concept which outperforms some previous designs found in the literature [4]-[8] in terms of size, improved broadside radiation, and reduced gain variation while also offering comparable wideband operation. To improve structure compactness when compared to [5], the size of the ground plane is reduced by almost 70% and a rated dielectric constant value of 30 is employed for the DR element (previous designs [4]-[8] used DR elements having a dielectric constant of about 10). In this work more importantly, a miniaturized slot ring element is also integrated within the compact ground plane which can improve radiation efficiency and operating bandwidth. Our fabricated and measured antenna exhibits a peak realized gain of 7.5 dBic at 1.45 GHz with a 3 dB axial ratio and half-power BW of more than 40%. The size of our proposed antenna structure, when compared to the wavelength at the highband (1.7 GHz), is $0.51\lambda_0$ by $0.51\lambda_0$ by $0.14\lambda_0$. Possible applications for the proposed DRA include satellite navigation and communication systems, wireless communications, in particular, where efficient wideband CP antenna operation and general structure compactness is required as well as high gain.

II. ANTENNA OPERATION, DESIGN, & ASSEMBLY

Our proposed DRA is defined by an arrangement of primary radiating ACSs having quadrature feeding [5], [9]. Degenerate radiating $HE_{11\delta}$ modes of the DR are excited by these four slots which are fed by 50-Ω microstrip transmission lines. The proposed cavity structure and the layout of the printed circuit board (PCB) for the antenna are shown in Figs. 1 and 2.

The inclusion of the meandered slot ring, which surrounds the DR, acts as an radiating element to improve gain and radiation efficiencies. This secondary radiating element is etched out of the top ground plane which defines the compact

This article has been accepted for publication in a future issue of this journal, but has not been fully edited. Content may change prior to final publication. Citation information: DOI 10.1109/LAWP.2015.2480547, IEEE Antennas and Wireless Propagation Letters

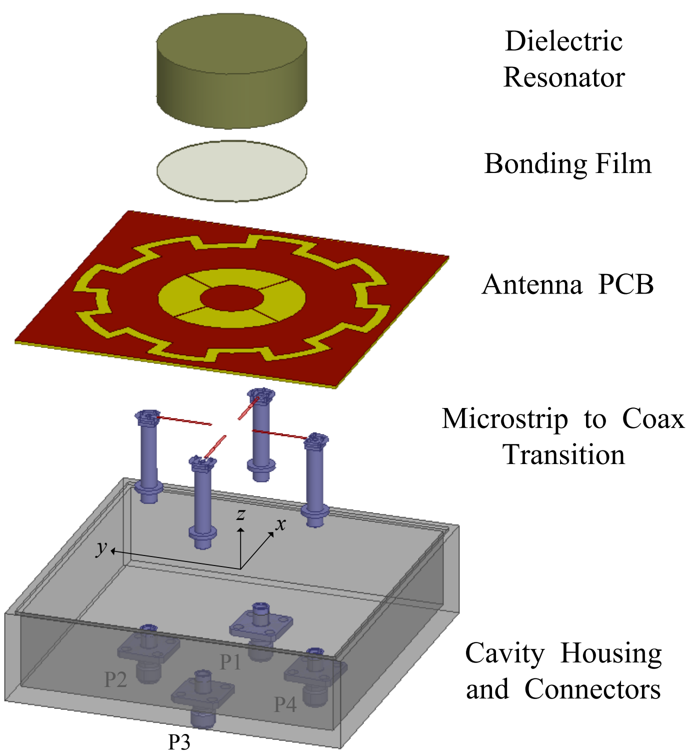

Fig. 1. Stackup of the cavity-backed antenna structure: cylindrical dielectric resonator, bonding film adhesive, two-layer printed circuit board (PCB), transition from microstrip to coax, cavity backing and SMA connectors.

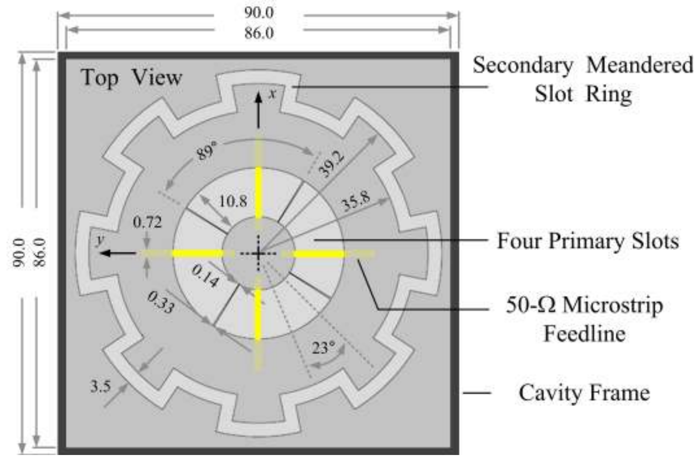

Fig. 2. Geometry for the PCB layout and the frame of the cavity (top view). All lengths and angles are provided in millimeters and degrees, respectively.

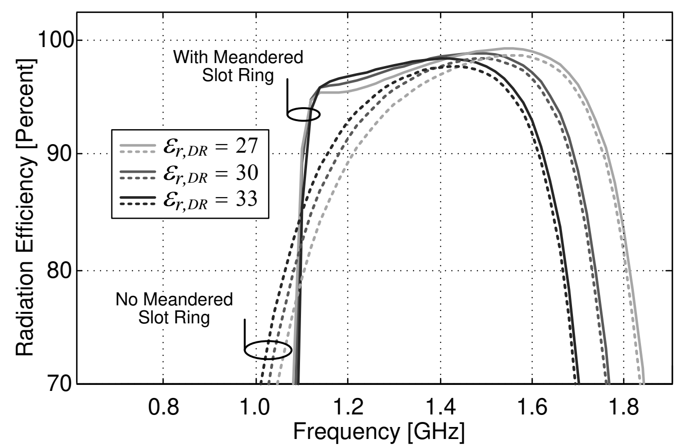

Fig. 3. Simulated radiation efficiency for the complete antenna (defined by all possible material losses, the feed system, and cavity as shown in Fig. 1).

PCB platform (86 mm by 86 mm) for the DR. Moreover, the cavity backing ensures radiation from the ring and the ACSs is directed into the top-side of the structure ($+z$-direction). Thus antenna operation is defined by the combined radiation of the ACSs within the PCB, the $HE_{11\delta}$ modes of the DR, and the radiation from the cavity-backed meandered slot ring.

A commercial full-wave simulation tool (Ansys HFSS [10]) was used to optimize the dimensions for the proposed compact antenna structure and an initial design goal was chosen to achieve the highest possible antenna gain over the widest possible BW while maintaining reduced reflection losses. More specifically, the dimensions for the PCB layout were optimized as well as the thickness and size of the cavity and the height of the cylindrical DR.

Assembly of the antenna unit included the bonding of a cylindrical DR (radius and height, 19.2 mm and 15.2 mm) with a high dielectric constant (Eccostock HiK500F, rated: $\varepsilon_{r,DR} = 30 \pm 10\%$) to a 31 mil thick, 86.0 mm by 86.0 mm PCB substrate (Taconic CER-10, rated: $\epsilon_{r,PCB} = 10$). The employed bonding film had a relative dielectric constant of approximately 10 (Loctite 383). As illustrated in Fig. 1 this PCB-DR component was then placed onto a square aluminum cavity structure (90.0 mm by 90.0 mm by 24.2 mm). Connectivity between the 50-Ω ports of the antenna and the microstrip lines of the PCB was achieved using a surface mount microstrip to coax transition (Gilbert/Corning, A012-P93-01), a bullet interconnect (Emerson Network Power Connectivity Johnson, 127-0901-811), and an SMA Jack (Pastenack, PE91061) positioned on the back side of the cavity. It should also be noted that a vertical connection through the cavity was required, versus a conventional feedline system that extends to the periphery of the PCB substrate. Moreover, the proposed antenna unit was designed and optimized such that the four coaxial feedlines were positioned appropriately as to not interfer with the field distributions located near the secondary slot ring.

III. Theoretical Considerations

The simulated radiation efficiency and the magnitude of the electric field within the PCB layer are shown in Figs. 3 and 4 with quadrature excitation for Ports 1 through 4. A comparison is made with and without the meandered slot ring. A parametric study of the radiation efficiency versus frequency is also reported for different and optimized structures with $\varepsilon_{r,DR} = 27$, 30, and 33, mainly to observe the possible frequency shift for the operating antenna BW. More specifically, to observe antenna operation as a result of the rated $\pm 10\%$ variance in the relative dielectric constant of the DR element.

It can be observed in Fig. 3 that similar radiation efficiencies are possible beyond 1.5 GHz. However, at 1.1 GHz, an improvement of about 10% can be observed with the secondary meandered slot ring. This radiation efficiency enhancement

This article has been accepted for publication in a future issue of this journal, but has not been fully edited. Content may change prior to final publication. Citation information: DOI 10.1109/LAWP.2015.2480547, IEEE Antennas and Wireless Propagation Letters

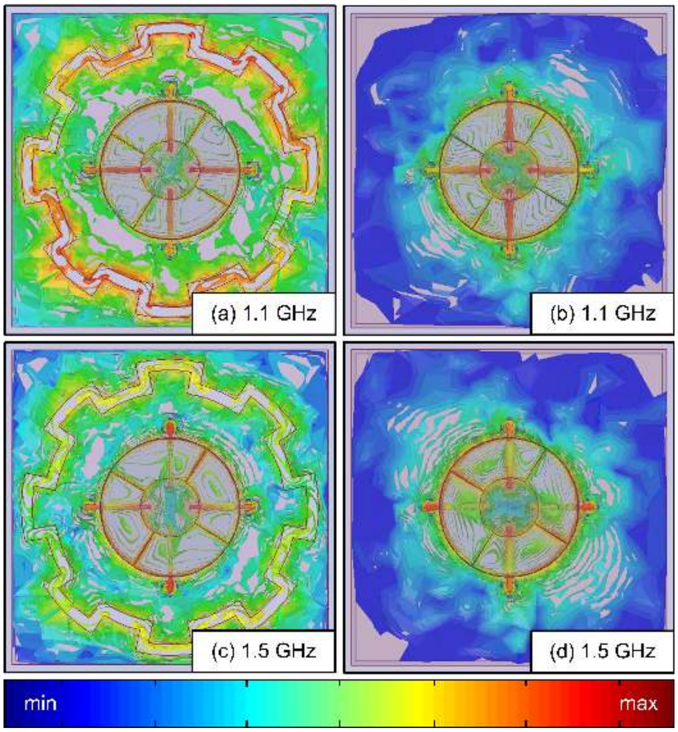

Fig. 4. Simulated magnitude of the electric field within the antenna PCB and with $\varepsilon_{r,DR}$ = 30: (a) and (c) with the meandered slot ring, (b) and (d) without the slot ring. Values shown in dB V/m and with a common scale. Similar results were observed for $\varepsilon_{r,DR}$ = 27 and 33.

is made possible for the antenna because the DR and ACSs generate a suitable electric field distribution within the PCB, as well as appropriate currents within the interior surface of the cavity and ground plane, to achieve excitation and resonance of the miniaturized slot ring for radiation at 1.1 GHz (see Fig. 4(a)). Moreover, the field distribution within the vicinity of the meandered slot ring has similarities to a cavity backed radial slot antenna and this field profile is comparable to a radiating mode for microstrip ring. As a result of this additional radiating element, realized antenna gain values (simulated, not shown) increased from -4.22 dBic to 3.88 dBic at 1.1 GHz.

Beyond 1.1 GHz, and within the operating band of the antenna, the meandered slot ring also acts as a secondary radiating element to improve total antenna efficiency. This is shown in Fig. 3. As illustrated in Fig. 4(c), antenna operation at 1.5 GHz can be defined by the hybridized radiation from the non-resonant slot ring as well as the DR and the microstrip fed aperture coupled slots. Conversely, for the comparative structure without the secondary ring (see Fig. 4(b) and (d)), the far-field beam patterns are generated by the PCB fields near the cylindrical DR and the primary slots only. As expected reduced radiation efficiency can be observed in Fig. 3 from 1.1 GHz to about 1.8 GHz.

IV. Measurement Results & Discussions

Upon fabrication and assembly the compact cavity-backed DRA was measured in the anechoic chamber facilities at The Royal Military College of Canada. Sequential 90° feeding of the ACSs was made possible by calibrated and phase matched

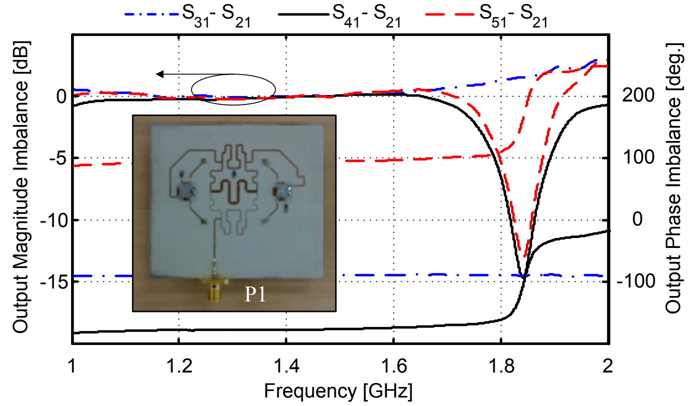

Fig. 5. Measurements of the five-port external feeding circuit used during antenna testing to achieve quadrature excitation of the ACSs. The input port (P1) is highlighted in the inset. Output ports (P2 through P5) are not visible.

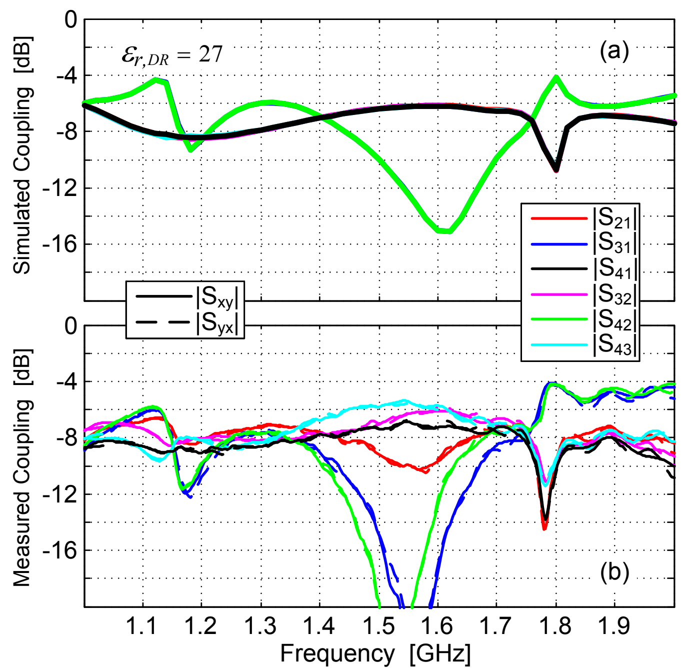

Fig. 6. Coupling between the SMA ports connected to the cavity backing of the antenna structure; i.e. P1, P2, P3, and P4 as described in Fig. 1.

cables as well as an external feed circuit (see Fig. 5 inset). This planar circuit was implemented by following [9], mainly to assist in the demonstration of our proposed antenna structure which was optimized for CP operation. Some results for this newly designed feeding circuit are reported in Fig. 5.

It should also be mentioned that after bonding the DR to the PCB antenna platform and affixing the cavity, port coupling measurements were completed and results are shown in Fig. 6. These measurements were studied to ensure connectivity between the SMA ports and the microstrip lines printed on the PCB backside. Also, given the rated variance specification for the DR element, $\varepsilon_{r,DR} = 30 \pm 10\%$, additional simulations were completed to estimate the relative dielectric constant of the DR (all results not shown for brevity). In particular, by comparing the simulated port coupling values for $\varepsilon_{r,DR} = 27$, 30, and 33 with the measurements, it was found that $\varepsilon_{r,DR} =$

This article has been accepted for publication in a future issue of this journal, but has not been fully edited. Content may change prior to final publication. Citation information: DOI 10.1109/LAWP.2015.2480547, IEEE Antennas and Wireless Propagation Letters

27 was a suitable estimate for the DR material.

Given this revised material value, which is different from the nominal value provided by the manufacturer, good agreement can be observed between the measurements and simulations for the port coupling values as well as the input matching of the antenna as shown in Figs. 6 and 7, respectively. As a result of this experiment, all simulation results provided in this section are those for a cylindrical DR having $\varepsilon_{r,DR} = 27$.

The aforementioned five-port external feed system was implemented using two 90° modular component hybrid couplers (Anaren model XC1400P-03S) and one compact 180° planar hybrid in microstrip technology [9]. Results in Fig. 5 were used to correct the antenna measurement values and ensure an adequate comparison with the simulations (which did not include the feed system). It should be noted that operation of the external feed system was limited to about 1.7 GHz. This is due to the rated frequency limitations of the modular 90° hybrids and the resultant output magnitude [phase] imbalance for the external circuit ports; i.e. $|S_{41}| - |S_{21}| < -5$ dB $[\angle S_{41} - \angle S_{21} > -90°]$ at 1.8 GHz as shown in Fig. 5. These practicalities can explain the reduction in the realized gain below 0 dBic at 1.7 GHz (see Fig. 7). Regardless of these facts, the designed external feed circuit provides the needed quadrature output and antenna measurements are in general agreement with the simulations as shown in Figs. 7 to 9.

The resulting antenna gain for right-handed circular polarization (RHCP) operation is reported in Fig. 7. Results are also shown versus the major antenna dimension, or the finite 90 mm size of the ground plane, d, compared to the free-space wavelength, λ_0. It can be observed that the fabricated CP antenna achieves a maximum gain of 7.5 dBic at 1.45 GHz, and by comparing this measured antenna gain (which includes mismatches) with respect to the pattern directivity at broadside, a radiation efficiency in excess of 90% can be evaluated. A relatively flat response is also shown for both the simulations and the measurements from 1.15 GHz to 1.55 GHz. These frequencies corresponds to ground plane lengths of $0.34\lambda_0$ and $0.46\lambda_0$ for the compact antenna structure, respectively.

Figure 8 plots the measured radiation pattern for the antenna at 1.40 GHz. Values are provided for both RHCP and left-handed circular polarization (LHCP) and results are in agreement with the simulations. Both the measured and simulated cross-polarization levels are quite low; i.e. values are 20 dB below the main beam maximum at broadside. Axial ratios are also provided in Fig. 9(a) as a function of frequency and in Fig. 9(b) at different beam angles in the $\phi = 0°$ plane. A worst case 3 dB axial ratio can be observed at 1.60 GHz from -90° to 118°. In addition, a 103° [115°] <159°> half-power beamwidth was measured at 1.15 GHz [1.40 GHz] <1.60 GHz>. These values are consistent with the simulations.

V. Conclusion

This work presented a miniaturized cavity-back dielectric resonator antenna (DRA) with the inclusion of a meandered circular slot ring which was etched out of the compact 90 mm by 90 mm ground plane of the antenna. Radiation efficiency values greater than 90% were reported and the -7 dB impedance BW of the DRA was measured to be 35% centered about 1.45 GHz. This center frequency corresponds to a free-space wavelength that is greater than 200 mm, which is more than double the length of the ground plane for the compact antenna. Additionally, a peak radiation gain of 7.5 dBic was observed with values in excess of 0 dBic from 1.13 GHz to 1.70 GHz. Physically speaking, excitation of the radiating $HE_{11\delta}$ modes of the dielectric resonator element generated surface currents on the compact ground plane and within the cavity such that the meandered slot ring can resonate and re-radiate these surface currents. It was also shown that our antenna can allow for improved radiation efficiency and BW when compared to a similar cavity-backed DRA which does not include this secondary meandered slot ring.

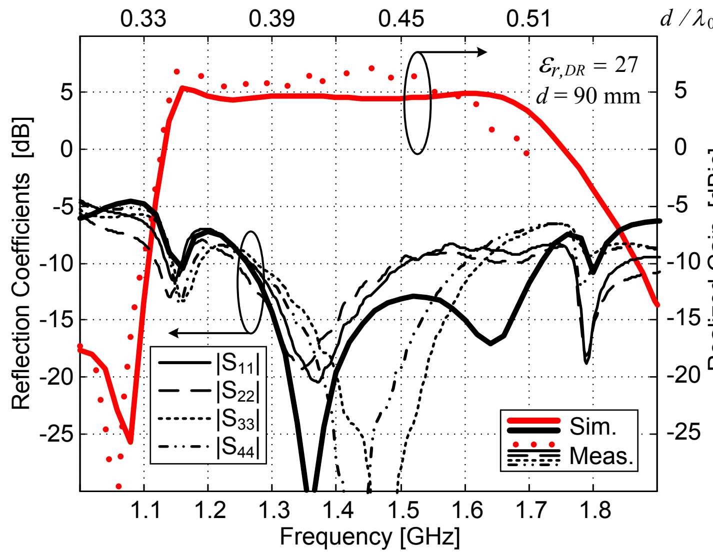

Fig. 7. The simulated (black solid line) and measured reflection coefficients (dashed/dotted lines) as well as the realized RHCP antenna gain at broadside. Small variations can be observed between the individually measured reflection coefficients. This is likely related to minor fabrication and assembly tolerances.

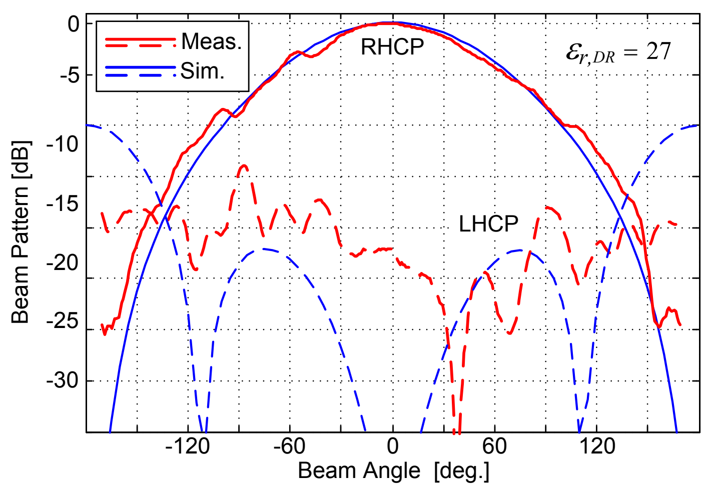

Fig. 8. Comparison of the measured and simulated RHCP beam patterns at 1.40 GHz in the $\phi = 0°$ plane. Also shown are the cross-polarization levels.

This article has been accepted for publication in a future issue of this journal, but has not been fully edited. Content may change prior to final publication. Citation information: DOI 10.1109/LAWP.2015.2480547, IEEE Antennas and Wireless Propagation Letters

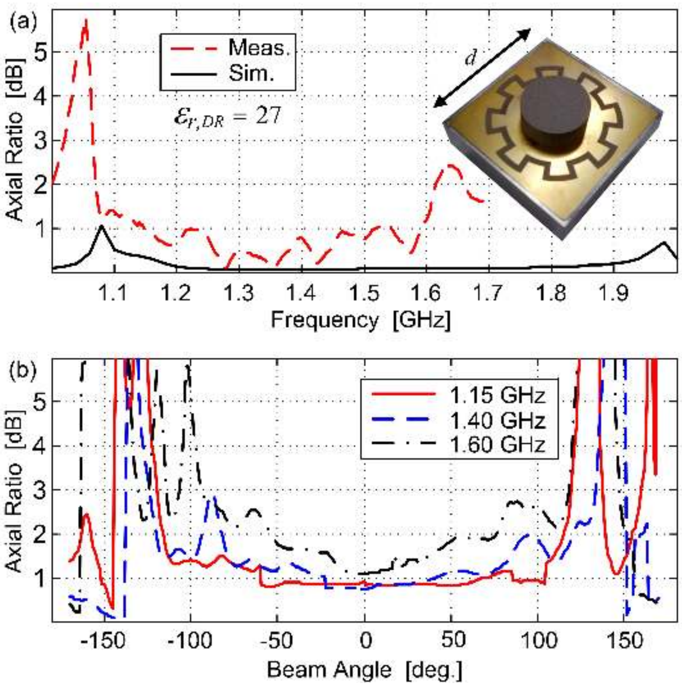

Fig. 9. (a): Axial ratio as a function of frequency at broadside. The fabricated antenna is shown in the inset. (b): Measured axial ratios versus beam angle.

REFERENCES

[1] K. M. Luk, and K. W. Leung, *Dielectric Resonator Antennas*, Research Studies Press, 2003.

[2] A. Petosa, *Dielectric Resonator Antenna Handbook*, Artech House, 2007.

[3] A.A. Kishk, and Y.M.M. Antar, *Dielectric Resonator Antennas* from J.L. Volakis: *Antenna Engineering Handbook*, Ch. 17, McGraw-Hill, 2007.

[4] K.W. Khoo, Y.X. Guo, and L.C. Ong, "Wideband circularly polarized dielectric resonator antenna, *IEEE Trans. Ant. Prop.*, vol. 55, no. 7, pp. 1953–1932, Jul. 2007.

[5] G. Massie, M. Caillet, M. Clénet, and Y. M. M. Antar, "A new wideband circularly polarized hybrid dielectric resonator antenna," *IEEE Ant. and Wireless Prop. Lett.*, vol. 9, pp. 347-350, 2010.

[6] Y. Pan and K.W. Leung, "Wideband circularly polarized trapezoidal dielectric resonator antenna," *IEEE Ant. and Wireless Prop. Lett.*, vol. 9, pp. 588-591, 2010.

[7] M.I. Sulaiman and S.K. Khamas, "A singly fed wideband circularly polarized dielectric resonator antenna using concentric open half-loops," *IEEE Ant. and Wireless Prop. Lett.*, vol. 10, pp. 1305-1308, 2011.

[8] M. Khalily, M.K.A. Rahim, and A. Kishk, "Planar wideband circularly polarized antenna design with rectangular ring dielectric resonator and parasitic printed loops," *IEEE Ant. and Wireless Prop. Lett.*, vol. 11, pp. 905-908, 2012.

[9] M. Caillet, M. Clénet, and Y. M. M. Antar, "Miniaturized broadband planar feeding systems for circularly polarized antennas," presented at the IEEE Eur. Conf. on Antennas and Propagation, Apr. 2011.

[10] "Ansys High Frequency Structure Simulator v. 15.0, ANSYS, Inc. 2015 [Online]. Available: www.ansys.com